The influence of droplet size and biodegradation on the transport of subsurface oil droplets

during the *Deepwater Horizon* spill: a model sensitivity study

Environmental Research Letters

LETTER

The influence of droplet size and biodegradation on the transport of subsurface oil droplets during the *Deepwater Horizon* spill: a model sensitivity study

Elizabeth W North[1], **E Eric Adams**[2], **Anne E Thessen**[3], **Zachary Schlag**[1], **Ruoying He**[4], **Scott A Socolofsky**[5], **Stephen M Masutani**[6] **and Scott D Peckham**[7]

[1] University of Maryland, Center for Environmental Science, Horn Point Laboratory, 2020 Horns Point Road, Cambridge, MD 21613, USA
[2] Massachusetts Institute of Technology, Department of Civil and Environmental Engineering, Rm 48-216b, Cambridge, MA 02139, USA
[3] The Data Detektiv, 1412 Stearns Hill Road, Waltham, MA 02451, USA; The Ronin Institute for Independent Scholarship, Montclair, NJ, USA
[4] North Carolina State University, Department of Marine, Earth and Atmospheric Sciences, 2800 Faucette Drive, Raleigh, NC 27695-8208, USA
[5] Texas A & M University, Zachry Department of Civil Engineering, Coastal and Ocean Engineering Division, 3136 TAMU, College Station, TX 77843-3136, USA
[6] University of Hawaii, Hawaii Natural Energy Institute, 1680 East West Road, POST 109, Honolulu, HI 96822, USA
[7] University of Colorado, INSTAAR, 4001 Discovery Drive, Boulder, CO 80303, USA

E-mail: enorth@umces.edu

Abstract

A better understanding of oil droplet formation, degradation, and dispersal in deep waters is needed to enhance prediction of the fate and transport of subsurface oil spills. This research evaluates the influence of initial droplet size and rates of biodegradation on the subsurface transport of oil droplets, specifically those from the *Deepwater Horizon* oil spill. A three-dimensional coupled model was employed with components that included analytical multiphase plume, hydrodynamic and Lagrangian models. Oil droplet biodegradation was simulated based on first order decay rates of alkanes. The initial diameter of droplets (10–300 μm) spanned a range of sizes expected from dispersant-treated oil. Results indicate that model predictions are sensitive to biodegradation processes, with depth distributions deepening by hundreds of meters, horizontal distributions decreasing by hundreds to thousands of kilometers, and mass decreasing by 92–99% when biodegradation is applied compared to simulations without biodegradation. In addition, there are two- to four-fold changes in the area of the seafloor contacted by oil droplets among scenarios with different biodegradation rates. The spatial distributions of hydrocarbons predicted by the model with biodegradation are similar to those observed in the sediment and water column, although the model predicts hydrocarbons to the northeast and east of the well where no observations were made. This study indicates that improvement in knowledge of droplet sizes and biodegradation processes is important for accurate prediction of subsurface oil spills.

1. Introduction

With the advent of technologies that allow oil recovery from hundreds of meters below the sea surface, a better understanding of oil droplet formation, evolution, transport, and degradation in deep waters is necessary to predict the fate and transport of subsurface oil spills (Yapa *et al* 2012). In addition, this information is

necessary to fully understand the impact of dispersants applied at the wellhead which greatly affects droplet sizes (Johansen *et al* 2013, Vilcáez *et al* 2013, Nagamine 2014) and to better constrain the estimate of the mass of initially suspended droplets in deep hydrocarbon plumes, which is one of the largest uncertainties in the hydrocarbon budget of the *Deepwater Horizon* (DH) spill (Ryerson *et al* 2012).

Figure 1. Video frame capture showing tip streaming from DH proxy crude oil mixed with COREXIT 9500 at 1:50 DOR during simulated buoyant rise: (a) original frame capture and (b) cropped and expanded. Buoyant droplets are stabilized for observation with a downward flow of synthetic seawater. Filaments of oil are shed from the edges of droplets (tip streaming) resulting in a rapid decrease in size. The width of the large crescent-shaped droplet is ~3 mm; it disappeared within 20–30 min, producing an ensemble of tiny droplets $< \sim 100\ \mu$m. See Nagamine (2014) for more details. Contrast of images was adjusted for clarity.

Although poorly constrained, the estimated mass of hydrocarbons in the form of oil droplets in the subsurface plume during the DH spill was significant. A total of $\sim 1.01 \times 10^7\,\mathrm{kg\,d^{-1}}$ of hydrocarbons was released (table S1 in Ryerson *et al* 2012) and 62% of the total released was oil (figure 1 in Ryerson *et al* 2011). Of that, $\sim 1.09 \times 10^6\,\mathrm{kg\,d^{-1}}$ of insoluble hydrocarbons were transported into the deep plume (table S1 in Ryerson *et al* 2012), which indicates that ~17.4% of the oil that was released from the well went into the subsurface plume in the form of oil droplets. For an 83-day spill, this totals ~665 000 barrels of oil, which is more than twice the size of the *Exxon Valdez* spill (US Coast Guard 1993).

Although there is strong evidence for the presence of subsurface plumes of dissolved hydrocarbons formed during the DH spill (Camilli *et al* 2010, Valentine *et al* 2010, Kessler *et al* 2011, Socolofsky *et al* 2011, Du and Kessler 2012), published observations of liquid oil droplets in these plumes are more limited (Loomis 2011, Reddy *et al* 2012, Weber *et al* 2012). Nevertheless, laboratory, field, and modeling experiments indicate that small droplets of oil could be

present in subsurface plumes in addition to dissolved hydrocarbon compounds (Johansen *et al* 2003, Yapa and Chen 2004, Nagamine 2014). Through extensive laboratory experiments, Brandvik *et al* (2013) describe droplet sizes resulting from the initial break-up of oil in highly energetic buoyant jets. A methodology to scale these measurements to the field scale, based on a modified Weber number, has been reported (Johansen *et al* 2013). The model by Johansen *et al* (2013) suggests that the initial droplet sizes were in the approximate range of 1–10 mm during periods when chemical dispersants were not used at the DH spill. Such relatively large sizes would have ascended to the surface in a period of hours, too short of a time for significant biodegradation in the water column. Chemical dispersants reduce the interfacial tension between oil and water and the same model suggests that, for the DH spill, dispersant-treated oil droplets were roughly ten times smaller, in the range of 100–1000 μm. The smaller droplets in this range could have entered the subsurface plumes (intrusion layers), outside of the main bubble/droplet plume (Chan *et al* 2014), and would have ascended over periods of up to 100 s of

hours. Additionally, observations by Nagamine (2014) and others suggest that chemical dispersants can cause significant reductions in oil droplet size after initial breakup through the processes of tearing and tip-streaming. Nagamine (2014) found that buoyant millimeter size crude oil droplets, mixed with dispersant at a dispersant to oil volume ratio (DOR) of 1:50 (i.e., 2% by volume) and stabilized in space in a downward-flowing water tunnel, evolved into an ensemble of droplets with diameters of $0.1–50\,\mu m$ after 8 h (see figure 1 for image of tip-streaming). In contrast, untreated oil droplets exhibited no noticeable changes over a period of 24 h. While a number of questions still remain regarding the effectiveness of chemical dispersants, such as the roles of temperature, the presence of gas mixed with oil, and the method by which dispersant and oil are mixed, it is clear that a wide range of droplet sizes is possible.

Numerical modeling research aimed at predicting the fate and transport of dissolved and liquid oil during the DH spill has revealed important influential factors, including the roles of droplet size and biodegradation (the consumption of hydrocarbons by microbes). Neutrally buoyant Lagrangian drifters at fixed depths have been used to demonstrate the importance of bathymetric steering (Weisberg *et al* 2011) and small-scale eddies (Chang *et al* 2011) on the potential transport of subsurface plumes. Three dimensional (3D) Lagrangian models also have been applied to simulate the DH spill, and indicate that oil droplets $\leqslant 80\,\mu m$ formed subsurface plumes (North *et al* 2011, Paris *et al* 2012), that the use of dispersants at the wellhead deepened the location of suspended oil mass (Paris *et al* 2012), and that biodegradation increased the residence time of oil in the water column (Lindo-Atichati *et al* 2014) and reduced the liquid and dissolved oil mass at similar rates to surface evaporation (Mariano *et al* 2011). Biodegradation was also found to be an important controller of the transport of dissolved subsurface hydrocarbons in an Eulerian study by Adcroft *et al* (2010). Dissolved hydrocarbons were predicted to stay within the northern Gulf of Mexico when biodegradation was included in the model parameterizations; when biodegradation was not included, the model predicted that hydrocarbons were transported to the Florida Straits and the Gulf Stream (Adcroft *et al* 2010). A 2D coupled physical-metabolic model indicated that subsurface mixing and circulation processes accelerated hydrocarbon degradation by bacteria through an autoinoculation effect (Valentine *et al* 2012). Although these studies point to the important role of biodegradation on the fate and transport of subsurface oil droplets, there are relatively few observations of *in situ* biodegradation rates in the deep (>1000 m) and cold ($<7\,°C$) waters of the Gulf of Mexico (Hazen *et al* 2010) and few laboratory studies of hydrocarbon biodegradation in seawater at these temperatures (Venosa and Holder 2007, Campo *et al* 2013, Prince *et al* 2013). In addition, the

interactive effects of initial droplet size and biodegradation rate on the spatial extent of oil droplet transport have not been quantified.

The objective of this study was to systematically assess the sensitivity of the 3D transport of subsurface oil droplets to biodegradation loss rates and initial droplet sizes. Toward this aim, a coupled 3D model was parameterized with a range of biodegradation rates and different initial oil droplet diameters. Coupled model predictions of the DH spill were examined to understand the influence of biodegradation loss rates on vertical and horizontal droplet distributions and hydrocarbon concentrations, and the potential interaction of oil droplets with the bottom. Observations of hydrocarbons in the subsurface and sediment were compared with model output in order to assess the validity of the predictions.

2. Methods

2.1. 3D coupled model

The 3D coupled model consisted of three components: (1) an analytical multiphase plume model to predict initial droplet depths (Socolofsky *et al* 2011), (2) the 3D South Atlantic Bight and Gulf of Mexico hydrodynamic model (SABGOM) to predict circulation patterns (Hyun and He 2010) and (3) the Lagrangian TRANSport model (LTRANS) to predict trajectories of oil droplets (North *et al* 2011). SABGOM and the multiphase plume model passed information to LTRANS and were not linked to each other. Oil droplet rise velocities in LTRANS were based on equations in Zheng and Yapa (2000). Oil droplet density was fixed at 858 kg m^{-3} (reported in Lehr *et al* (2010) and used by Socolofsky *et al* (2011)). Dynamic viscosity was determined after interpolating SABGOM salinity and temperature to the droplet location. More information about the three model components can be found in the supplementary material (S1.Text) available at stacks.iop.org/ERL/10/024016/mmedia. This 3D coupled model successfully predicted that oil droplets $10–50\,\mu m$ in diameter occurred at the same time and location as the southwest-tending plume of hydrocarbons which was observed by Camilli *et al* (2010) during the DH spill (North *et al* 2011).

2.2. Oil droplet biodegradation

Oil droplet biodegradation was simulated by decreasing the diameter of oil droplets based on observed first-order biodegradation rates of alkanes. Dissolution was neglected; it was assumed that the bulk of the dissolution of the lighter hydrocarbons occurred in the buoyant plume and that mass-loss processes in the far field were dominated by biodegradation-mediated processes. To simulate oil droplet biodegradation in LTRANS, we applied a first order decay rate of mass (M) to shrink droplet diameters (D) based on the relationship between diameter and mass $\left(M = \frac{\rho\pi}{6}D^3 \right)$.

We explicitly assumed droplets were spherical, remained at constant density (ρ) during biodegradation, and that all droplets in the simulation had the same decay rates. We thus neglected any spatial gradients of bacterial concentration or any biofilm that may have coated the droplets after colonization. The size at which droplets dissolved was defined as $0.19 \, \mu m$, the size that would pass through a $0.2 \, \mu m$ glass fiber filter, which is an operational definition for a dissolved substance. With density held constant, this analysis isolated the sensitivity of predicted transport based on changes in droplet diameter alone.

The biodegradation rates of oil droplets, most likely due to the activities of *Colwellia* sp. of bacteria (Bælum *et al* 2012, Redmond and Valentine 2012), were parameterized with the decay rates for alkanes that Hazen *et al* (2010) observed in the DH subsurface plume that occurred at 5 °C. Hazen *et al* (2010) estimated biodegradation rates of C13–C26 *n*-alkanes from the field and from laboratory microcosms by fitting first order rate equations for exponential decay. Their minimum (1.2 *d*) and maximum (6.1 *d*) half-lives were used to parameterize oil droplet biodegradation in 'fast' and 'slow' biodegradation rate scenarios for the simulations here. In addition, an 'average' half-life of 3.05 *d* was simulated, which was the mean of the average half-lives from table S7 in Hazen *et al* (2010). These half-lives were within the range of biodegradation rates reported for alkanes at similar temperatures in laboratory studies (Venosa and Holder 2007, Campo *et al* 2013, Prince *et al* 2013).

2.3. Model simulations

To examine the sensitivity of oil droplet transport on biodegradation rates, model simulations were conducted with the three biodegradation rates (slow, average, and fast) using five different initial droplet diameters: 10, 30, 50, 100 and 300 μm, consistent with the above discussion of droplet sizes for dispersant treated oil. Simulated droplets were released in a continuous stream at the location of the DH spill (28.738°N, 88.366°W) from 22 April 2010 to 15 July 2010. The depth of droplet release varied with trap height estimated by the analytical multiphase plume model (Socolofsky *et al* 2011); LTRANS started tracking the droplets at the trap height because they no longer had a buoyant group effect and rose according to their density and diameter alone. The number of droplets released per time step was proportional to the time-varying flow rate of unrecovered oil from the well (McNutt *et al* 2011). In addition to 15 simulations with oil droplet biodegradation (three biodegradation rates x five initial droplet diameters), five simulations, each with a different initial droplet diameter, were conducted with no biodegradation as a baseline. A total of 81 609 droplets were tracked in each simulation which ended on 28 July 2010. Reflective boundary conditions were maintained to ensure robust simulation of the long term fate of the mass of oil represented by each particle.

Model results were compared to examine the influence of biodegradation rate on the horizontal and vertical transport of oil droplets. To reduce the complexity of the unsteady, evolving model solution and to analyze the long-term effects of biodegradation on the model results, model predictions were analyzed at a single point in time on 3 July 2010 (73 days after the start of the spill). Model predicted fields of both droplet distribution and hydrocarbon concentration were considered. Droplet numbers were converted to oil concentrations using the known discharge rate of unrecovered oil from the well and the droplet volumes. For this purpose, droplets in the slow rising size range of 10–50 μm were assumed to constitute 17.4% of the released oil—5.8% each in class of 10, 30 and 50 μm (see section 1 for calculation of 17.4%). Analyses of hydrocarbon concentrations were made for fast, average, slow, and no biodegradation rate simulations to examine model sensitivities.

Model results also were examined to assess the influence of droplet size and biodegradation rates on the potential interaction of oil droplets with the seafloor. The index of potential interaction ('bottom hits' per km^2) was calculated by keeping track of the location that droplets reflected off the bottom during the 98-*d* simulations. Bottom hits per km^2 were calculated as the cumulative number of times droplets reflected off of the bottom in 25 km^2 areas during the 98-*d* model run, which was simply an index of the potential for subsurface oil droplets to interact with the bottom. Bottom hits per km^2 was not a prediction of the amount of oil that was present in bottom sediments because many important processes that govern oil sorption to the bottom were not taken into account.

2.4. Comparison with observations

To compare model predictions with observations, hydrocarbon data from the water column and the sediments were gathered from the Gulf Integrated Spill Research (GISR) Deepwater Horizon database (Thessen *et al* 2014, http://gisr.hpl.umces.edu). The database contains oceanographic and hydrocarbon data from 38 individual data sets collected by academia, industry and government in the northern Gulf of Mexico in 2010 and 2011. Data from the water column and sediments that were integrated within the GISR Deepwater Horizon database were retrieved via an SQL query. The specific analytes of interest were the hydrocarbons listed in table S2 of Reddy *et al* (2012) that characterize hydrocarbons released from the DH well. Comparisons were made between observations and model-derived bottom hits per km^2 because bottom hits per km^2 provided an integrated summary of the location of particles over the 98-*d* simulation. Bottom hits per km^2 were compared with:

(1) Observations of all hydrocarbons listed in table S2 of Reddy *et al* (2012) in the water column that were deeper than 200 m between the dates of 5/3/2010 and 12/19/2010 ($n = 390\,738$) to compare model predictions with all locations where subsurface hydrocarbons were measured and detected. Data sources: Reddy *et al* (2012), CSIRO (2013), Joung and Shiller (2013), NOAA/NOS (2013), ERMA (2014).

(2) Observations of *n*-C24 to *n*-C31 alkanes in the water column that were deeper than 700 m between the dates of 6/2/2010 and 10/16/2010 ($n = 12\,156$) to compare model predictions with the locations where slowly degrading alkanes were measured and detected. In addition, observations of benzene were analyzed to determine the last day on which benzene was detected deeper than 200 m ($n = 4905$) in order to determine if samples were enriched in *n*-C24 to *n*-C31 alkanes relative to benzene, which is an indicator of liquid oil droplets (Reddy *et al* 2012). Data sources: Lee and Ryan (2010), CSIRO (2013), NOAA/NOS (2013).

(3) Observations in the sediment of *n*-C10–11 ($n = 66$), *n*-C20–24 ($n = 169$), and *n*-C33–35 alkanes ($n = 99$) from 8/15/2010 to 9/30/2010 and of sodium 1,4-bis(2-ethylhexoxy)-1,4-dioxobutane-2-sulfonate (common name, dioctyl sulfosuccinate or DOSS) from 1/25/2011 to 6/11/2011 ($n = 505$) to compare model prediction with the location of compounds with fast (*n*-C10–11), slow (*n*-C20–24), and very slow degradation (*n*-C33–35, DOSS) at 5 °C (Kujawinski *et al* 2011, Campo *et al* 2013). Data sources: Reddy *et al* (2012), CSIRO (2013), Joung and Shiller (2013), NOAA/NOS (2013), ERMA (2014).

3. Results

Model results indicate that, for the range in initial droplet sizes considered, the transport of oil droplets was highly sensitive to oil biodegradation rates, with depth distributions deepening by hundreds of meters and horizontal distributions decreasing by hundreds to thousands of kilometers when biodegradation was applied (figure 2, table 1, S1.animation and S2.animation in supplementary material). For example, for droplets with initial diameters of 100 μm, the average depth deepened by 834 m, the maximum north–south distance between oil droplets decreased by 670 km, and the maximum east–west distance between oil droplets decreased by 1283 km when the fast degradation rate was applied compared to no biodegradation after 73 *d* of model simulation (table 1). These decreases in depth and distance were less pronounced for scenarios with 30 and 300 μm droplets, although decreases in depth of tens to hundreds of meters and decreases in distances by

hundreds of kilometers were predicted (table 1). The marked differences in horizontal and vertical transport between model runs was related to how long a droplet remained before becoming 'dissolved'; oil droplets with half-lives of 6.1 *d* persisted for >80 days longer than those with half-lives of 1.2 days (table 2). Initial droplet diameters also influenced model predictions. In all scenarios, oil droplets with 300 μm initial diameter rose rapidly to the surface and remained there, whereas those with 30 μm initial diameter were found mostly in the subsurface after 73 days (figure 2).

Hydrocarbon concentrations based on droplets with initial diameters of 10, 30 and 50 μm showed similar sensitivity to oil droplet biodegradation rates in horizontal and vertical distributions. Under fast biodegradation, no hydrocarbons were predicted in the upper 600 m 73 days after the spill and the distribution in the subsurface was limited (figure 3(a)). In contrast, oil droplets with average and slow biodegradation rates resulted in a wider predicted distribution of hydrocarbons in the subsurface, with a larger amount reaching mid-depths (400–600 m) and near surface waters (<200 m) (figures 3(b) and (c)). Slow biodegradation rates resulted in deep (1000–1200 m) hydrocarbon concentrations that had similar distributions as those with no biodegradation rates. In contrast, hydrocarbon distributions with no biodegradation (figure 3(d)) had higher concentrations in mid-depth and, especially, near-surface waters with a wider horizontal distribution that included transport of hydrocarbons to the Florida Straits. In all scenarios, hydrocarbon concentrations were estimated to be $>0.01\,\mu g\,l^{-1}$ (ppb) at select locations between 1000 and 1200 m. The difference in the concentration of hydrocarbons between the simulations in figure 3 was due to reduction in mass due to biodegradation. With no biodegradation, 100% of the mass remained within the model domain at day 73, whereas 1.5, 3.9 and 8.4% of the mass was left when fast, average, and slow biodegradation rates of alkanes were applied, respectively (table 3).

Potential interaction of oil droplets with the bottom was also markedly influenced by biodegradation rates. With no biodegradation, oil droplets with 100 and 300 μm initial diameters were not predicted to interact with the bottom until near shore because droplets rose rapidly to the surface (figures 4(h) and (l)). In contrast, bottom contact for these size droplets occurred in large regions on the shelf (300 μm) and shelf/slope (100 μm) when biodegradation rates were applied because their ascent rates were slower, allowing more time to interact with the bottom in the slope/shelf region (figures 4(f), (g), (j) and (k)). On the other hand, fast biodegradation rates led to a reduced footprint of potential interaction with the bottom (figures 4(a), (e) and (i)), limiting bottom interactions to the slope in waters 200–2000 m deep for 30 and 100 μm initial diameter droplets, because droplets dissolved before extensive interaction with the bottom
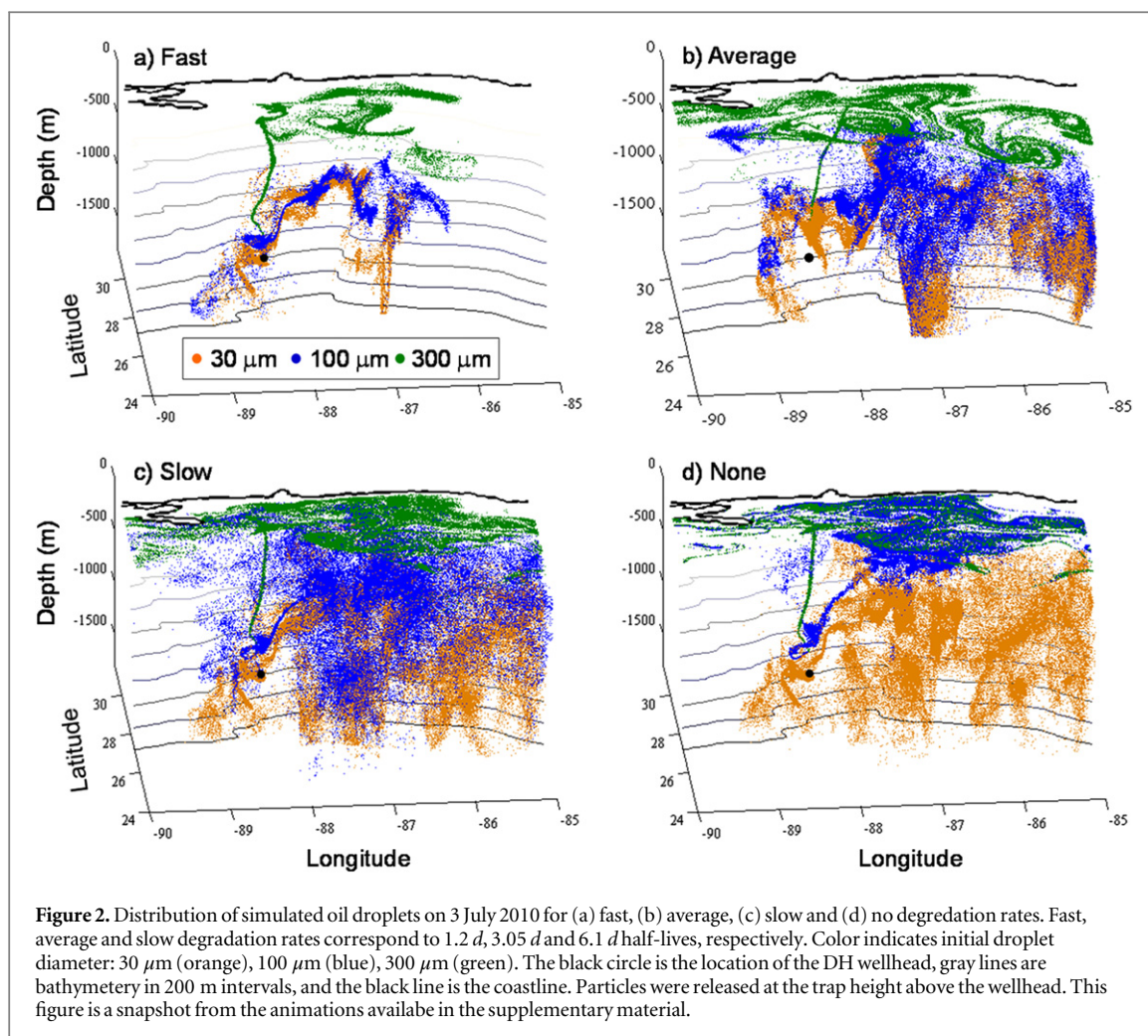
Figure 2. Distribution of simulated oil droplets on 3 July 2010 for (a) fast, (b) average, (c) slow and (d) no degradation rates. Fast, average and slow degradation rates correspond to 1.2 *d*, 3.05 *d* and 6.1 *d* half-lives, respectively. Color indicates initial droplet diameter: 30 μm (orange), 100 μm (blue), 300 μm (green). The black circle is the location of the DH wellhead, gray lines are bathymetery in 200 m intervals, and the black line is the coastline. Particles were released at the trap height above the wellhead. This figure is a snapshot from the animations availabe in the supplementary material.

Table 1. Depth and distance summary statistics for oil droplets with initial diameters of 30, 100 and 300 μm at day 73 of the model runs. Information about the model runs is included (initial diameter of droplets), the name of the biodegradation rate simulation, and the half-life employed. The statistics include minimum, maximum, and average depth (m) of oil droplets as well as the maximum north–south and east–west distance (km) between droplets in each simulation. Oil droplets were released between 1123 and 1173 m. Droplets with initial diameters of 300 μm rose to the surface whereas those with smaller initial diameters were transported both shallower and deeper of the release location.

Initial diameter (μm)	Degradation rate	Half-life (*d*)	Minimum depth of oil droplets (m)	Maximum depth of oil droplets (m)	Average depth of oil droplets (m)	Maximum north–south distance between oil droplets (km)	Maximum east–west distance between oil droplets (km)
30	Fast	1.2	393	2621	1145	290	354
30	Average	3.05	134	2948	1058	577	544
30	Slow	6.1	120	3000	1027	549	521
30	None	0	12	2725	895	957	552
100	Fast	1.2	158	2379	946	320	452
100	Average	3.05	41	2863	741	937	785
100	Slow	6.1	0	2805	505	1013	1361
100	None	0	0	1229	112	990	1735
300	Fast	1.2	0	1173	39	726	1646
300	Average	3.05	0	1173	27	1037	1944
300	Slow	6.1	0	1173	19	1019	1949
300	None	0	0	1173	16	992	1983

was possible. In simulations with 30 μm initial diameter droplets, the area with bottom hits >10 km^{-2} (10 droplets reflecting off bottom per km^2) was four times smaller in the fast biodegradation scenario than

the area in the average and slow biodegradation scenarios (table 3). In simulations with 100 μm initial diameter droplets, the area contacted by bottom hits >10 km^{-2} was two to four times smaller in the fast

Table 2. Size of initial simulated droplets, initial ascent speeds, and time to shrink from the initial droplet size to 0.19 μm, the size at which a droplet was considered to be dissolved, given a specified half-life ($t_{1/2}$).

Initial diameter (μm)	Ascent speed (cm s^{-1})	Time to dissolution (d)		
		$t_{1/2} = 1.2\,d$	$t_{1/2} = 3.05\,d$	$t_{1/2} = 6.1\,d$
10	0.0006	21	52	105
30	0.006	26	67	134
50	0.02	29	74	147
100	0.06	33	85	165
300	0.5	38	97	194

biodegradation scenario than the slow and average scenarios (table 3). All simulations with biodegradation and with 30 and 100 μm initial diameter droplets predicted potential interaction with the bottom southwest, southeast, and northeast of the DH site, including within De Soto canyon.

Bottom hits, the integrated footprint of hydrocarbons on the sediment over time, showed qualitative agreement with observations made to the southwest in water deeper than 200 m (figure 5) and in the sediment during and after the DH spill (figure 6, see also Montagna *et al* 2013). Observations of *n*-C24 to *n*-C31 alkanes in this southwest region were enhanced relative to benzene (figure 5(c)) which is an indicator that liquid oil droplets persisted in the subsurface (Reddy *et al* 2012) where this model predicted them. Few water column and sediment measurements of

Figure 3. Estimated hydrocarbon concentrations on 3 July 2010 at selected depths (0–200, 400–600, 1000–1200 m) when oil droplets were subject to (a) fast, (b) average, (c) slow and (d) no biodegradation rates. Hydrocarbon concentrations (μg l^{-1} or ppb) are the sum of droplet concentrations resulting from the distributions of droplets with initial diameters of 10, 30 and 50 μm, assuming that a total of 17.4% of the oil released from the *Deepwater Horizon* spill went into these size classes. The black diamond in each panel is the location of the DH wellhead.
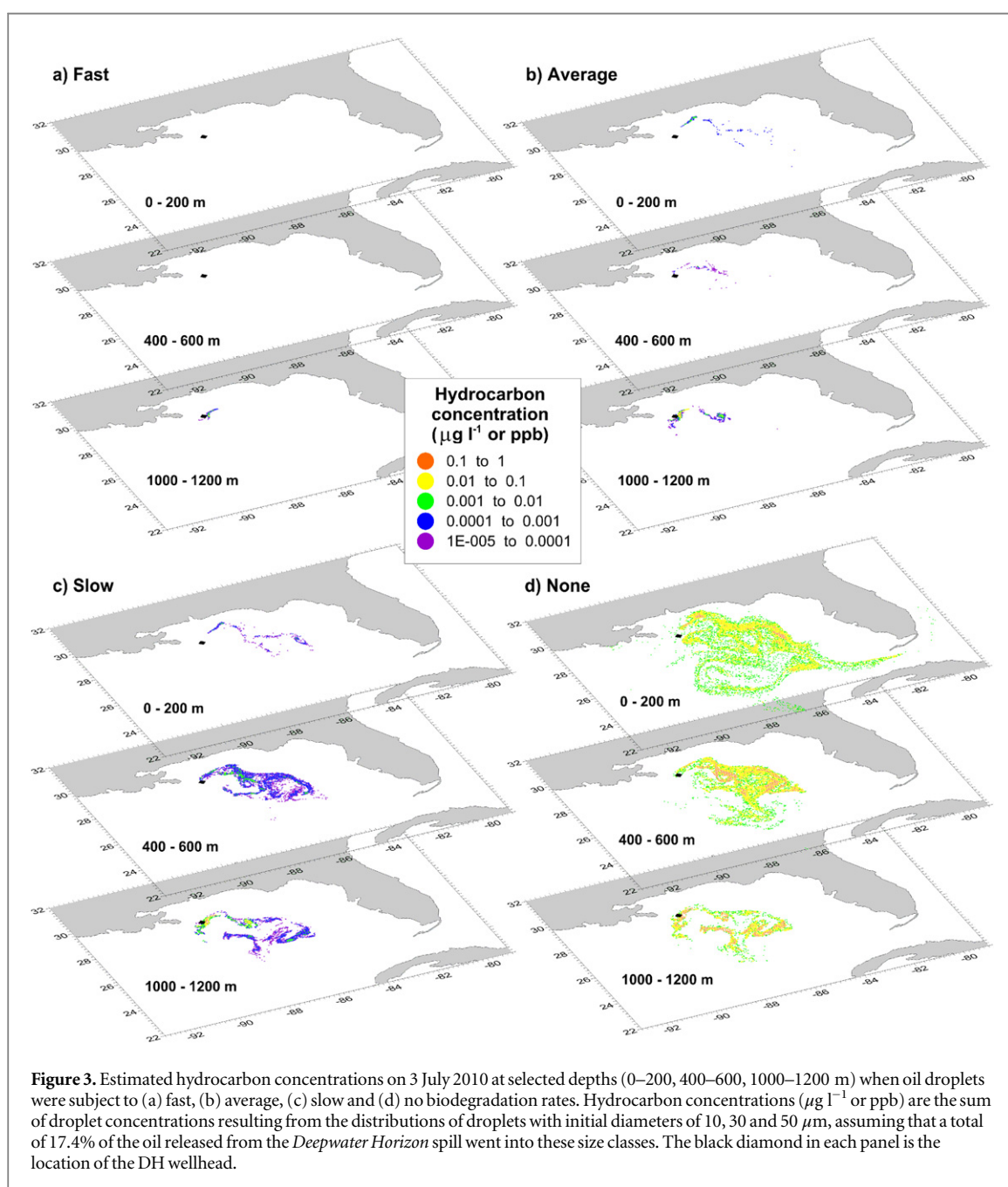
Table 3. Mass and area summary statistics for oil droplets with initial diameters of 30 and 100 μm which remained in the subsurface during model runs. Information about the model runs is included (initial diameter of droplets, the name of the biodegradation rate simulation, and the half-life employed). The statistics include the percent of mass remaining in each simulation at day 73 and 98 as well as the area of the continental slope (depth >200 m) which had bottom hits >10 km^{-2} at day 98.

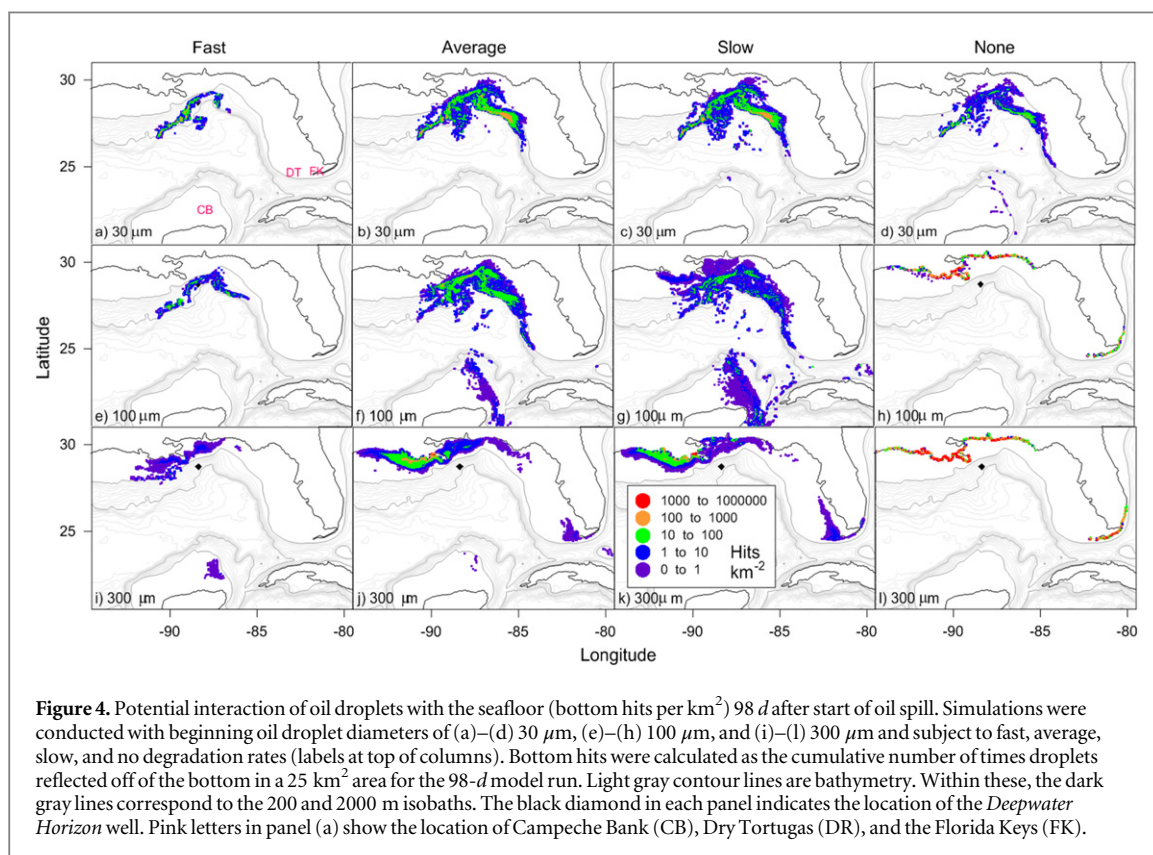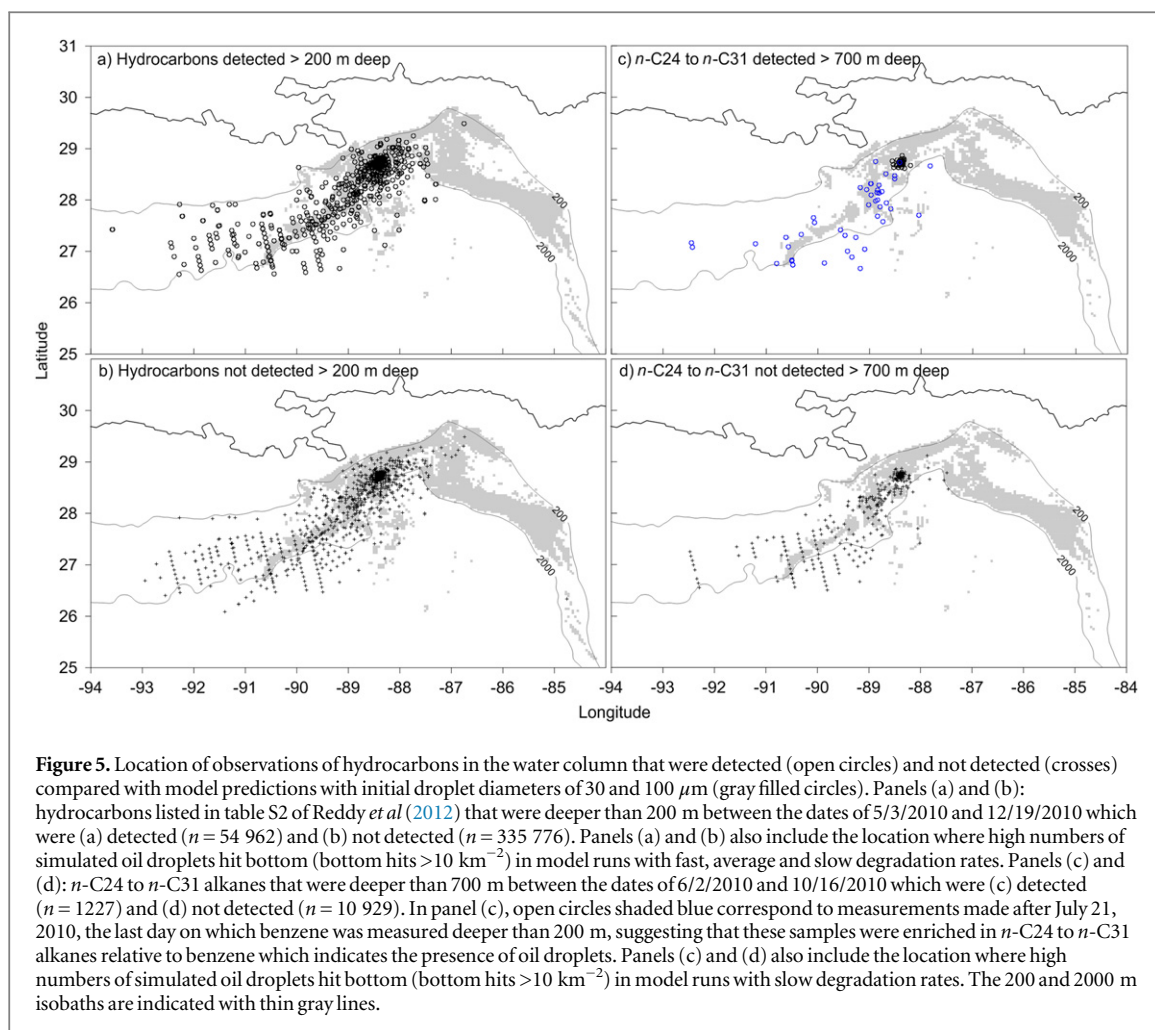| Initial diameter (μm)	Degradation rate	Half-life (d)	Percent mass remaining at day 73	Percent mass remaining at day 98	Slope area with bottom hits >10 km^{-2} (km^2)
30	Fast	1.2	1.5	0.0005	9225
30	Average	3.05	3.9	0.2	41 200
30	Slow	6.1	8.4	1.5	40 000
30	None	0	100	100	12 675
100	Fast	1.2	1.5	0	5400
100	Average	3.05	3.9	0.2	29 875
100	Slow	6.1	8.4	1.5	11 700
100	None	0	100	100	n/a

Figure 4. Potential interaction of oil droplets with the seafloor (bottom hits per km^2) 98 d after start of oil spill. Simulations were conducted with beginning oil droplet diameters of (a)–(d) 30 μm, (e)–(h) 100 μm, and (i)–(l) 300 μm and subject to fast, average, slow, and no degradation rates (labels at top of columns). Bottom hits were calculated as the cumulative number of times droplets reflected off of the bottom in a 25 km^2 area for the 98-d model run. Light gray contour lines are bathymetry. Within these, the dark gray lines correspond to the 200 and 2000 m isobaths. The black diamond in each panel indicates the location of the *Deepwater Horizon* well. Pink letters in panel (a) show the location of Campeche Bank (CB), Dry Tortugas (DR), and the Florida Keys (FK).

hydrocarbons were made to the northeast and east where the model predicted oil droplet transport (figures (5) and (6)), so comparison between model predictions and observations was not possible in this area. Although the model predicted bottom hits in the Dry Tortugas, Campeche Bank and the Florida Keys (figures 4(f), (g), (j) and (k)), no hydrocarbon accumulations have been recorded in these areas to our knowledge, although increased incidence of fish lesions related to hydrocarbons was observed near the Dry Tortugas (Murawski *et al* 2014, Weisberg *et al* 2014). It is highly likely that the model over-predicted transport to these far locations because other transformation processes besides biodegradation (e.g., dissolution) were not included in the model parameterization.

4. Discussion

The results of this sensitivity analysis clearly demonstrate that understanding biodegradation processes is crucial for accurate prediction of the dispersal of subsurface oil droplets. This is particularly true for chemically dispersed oil whose initial droplet sizes are small enough that the oil stays submerged for significant periods of time. Marked sensitivity to biodegradation also has been found in Eulerian (Adcroft *et al* 2010) and Lagrangian model frameworks (Lindo-Atichati *et al* 2014). Adcroft *et al* (2010) showed that predictions of transport with decaying oil were confined to the northern Gulf of Mexico whereas predictions with non-decaying oil resulted in transport to the Florida Straits and Gulf Stream. Our results are similar and indicate that biodegradation can decrease

Figure 5. Location of observations of hydrocarbons in the water column that were detected (open circles) and not detected (crosses) compared with model predictions with initial droplet diameters of 30 and 100 μm (gray filled circles). Panels (a) and (b): hydrocarbons listed in table S2 of Reddy *et al* (2012) that were deeper than 200 m between the dates of 5/3/2010 and 12/19/2010 which were (a) detected ($n = 54\,962$) and (b) not detected ($n = 335\,776$). Panels (a) and (b) also include the location where high numbers of simulated oil droplets hit bottom (bottom hits >10 km^{-2}) in model runs with fast, average and slow degradation rates. Panels (c) and (d): n-C24 to n-C31 alkanes that were deeper than 700 m between the dates of 6/2/2010 and 10/16/2010 which were (c) detected ($n = 1227$) and (d) not detected ($n = 10\,929$). In panel (c), open circles shaded blue correspond to measurements made after July 21, 2010, the last day on which benzene was measured deeper than 200 m, suggesting that these samples were enriched in n-C24 to n-C31 alkanes relative to benzene which indicates the presence of oil droplets. Panels (c) and (d) also include the location where high numbers of simulated oil droplets hit bottom (bottom hits >10 km^{-2}) in model runs with slow degradation rates. The 200 and 2000 m isobaths are indicated with thin gray lines.
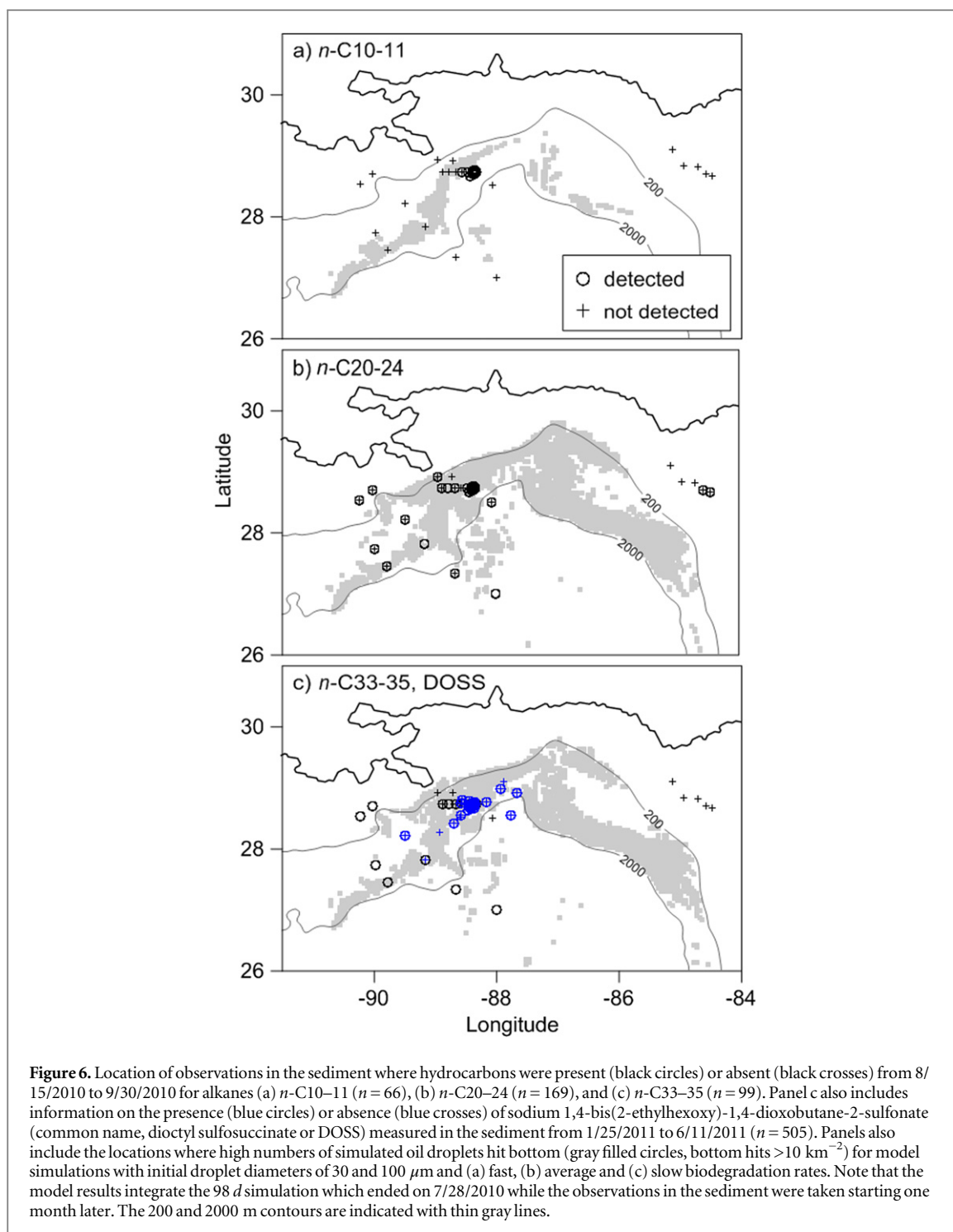
predictions of the horizontal spread of oil droplets by hundreds to thousands of kilometers.

In addition to affecting the horizontal transport of oil droplets, biodegradation also influenced the vertical transport of oil droplets and resulting hydrocarbon concentrations. Without biodegradation, our previous study suggested that droplets with diameters $\leqslant 80\,\mu$m formed subsurface plumes (North *et al* 2011). Results of this study suggest that droplets with initial diameters $\leqslant 100\,\mu$m which undergo fast biodegradation rates, and therefore experience slower ascent rates over time due to shrinkage, also could form subsurface plumes (figure 2(a)). Lindo-Atichati *et al* (2014) found that simulated droplets of up to 50 μm in diameter were near-neutrally buoyant and formed a persistent plume; differences in simulated biodegradation and the time scale of comparison could account for the difference in our findings and that of Lindo-Atichati *et al* (2014). In this study, the concentrations of hydrocarbons in the water column differed markedly between simulations when biodegradation rates of alkanes were and were not applied (figure 3) corresponding with a $>92\%$ reduction in mass in simulations with biodegradation after 73 *d*. In simulations without biodegradation, hydrocarbons concentrations in the 0–200 m depth interval were 10 to >1000

times higher than those with biodegradation because non-decaying droplets were able to accumulate near surface whereas the slowly-rising droplets subject to biodegradation diminished before reaching the upper layer. Due to the high sensitivity of oil droplet dispersal to biodegradation rates, prediction of the fate and transport of subsurface oil droplets would benefit from observations of biodegradation rates *in situ* in deep (>500 m) and cold (<7 °C) waters to confirm and enhance model parameterizations based on laboratory experiments as in this study and Lindo-Atichati *et al* (2014) or on microbial respiration as in Valentine *et al* (2012).

Our model results suggest that subsurface plumes of oil droplets could have directly interacted with the bottom, especially in the slope region, and that the extent of this interaction is sensitive to biodegradation processes (figure 4). Analysis of observations of 17α (H), 21β(H)-hopane in the sediment (Valentine *et al* 2014) supports our prediction that subsurface plumes of oil droplets contacted the bottom. In addition, the distributions of hydrocarbons predicted by our model were similar to those observed in the sediment and water column southwest of the well, although the model predicts hydrocarbons to the northeast and east of the well where no observations

Figure 6. Location of observations in the sediment where hydrocarbons were present (black circles) or absent (black crosses) from 8/15/2010 to 9/30/2010 for alkanes (a) n-C10–11 ($n = 66$), (b) n-C20–24 ($n = 169$), and (c) n-C33–35 ($n = 99$). Panel c also includes information on the presence (blue circles) or absence (blue crosses) of sodium 1,4-bis(2-ethylhexoxy)-1,4-dioxobutane-2-sulfonate (common name, dioctyl sulfosuccinate or DOSS) measured in the sediment from 1/25/2011 to 6/11/2011 ($n = 505$). Panels also include the locations where high numbers of simulated oil droplets hit bottom (gray filled circles, bottom hits >10 km^{-2}) for model simulations with initial droplet diameters of 30 and 100 μm and (a) fast, (b) average and (c) slow biodegradation rates. Note that the model results integrate the 98 d simulation which ended on 7/28/2010 while the observations in the sediment were taken starting one month later. The 200 and 2000 m contours are indicated with thin gray lines.

were made (figures (5) and (6)). Lindo-Atichati *et al* (2014) also predicted intersection of simulated subsurface plumes with the bottom, especially within Mississippi Canyon. It remains to be seen if evidence will surface to confirm or refute predictions of bottom deposition of oil along the slope near the Florida self. Nevertheless, the lack of observations in regions where models predicted subsurface oil suggests that incorporating 3D oil droplet models into response efforts for subsurface oil spills could be used to help inform sampling campaigns in the future and provide information to evaluate and improve model skill.

As noted by Camilli *et al* (2010) and Weisberg *et al* (2011), the importance of bathymetric steering on the subsurface plumes can be clearly seen in our model results, both in terms of the predicted location of deep hydrocarbon concentrations (figure 3) and oil droplet interaction with the bottom (figure 4). The understanding that plumes of subsurface oil droplets may contact the bottom at locations tens to hundreds of kilometers away from the site of deep water spills is an important concept for monitoring and mitigating the impacts of spills. The near-neutrally buoyant nature of these plumes enables them to be carried long distances

before they intersect with continental slopes. In addition, because no sedimentation processes were parameterized in the model, results indicate that contact of near-neutrally buoyant oil droplets with the bottom could result from hydrodynamics (advection and turbulence) alone.

Although there are several limitations of the model parameterization, they do not detract from our overall finding regarding the sensitivity of predictions of oil droplet dispersal to biodegradation. One limitation of this study is the use of a single hydrodynamic model; using an ensemble of models likely would be more robust and result in different particle distributions. Another limitation is the assumption that the density of the droplets do not change as the mass decreases and size diminishes over time. Droplets likely increase in density over time (although perhaps not shrink as fast) as lower molecular weight compounds are degraded first, which would tend to keep droplets in the subsurface for longer periods, which would likely increase predictions of bottom contact and dispersal. However, near neutrally-buoyant biofilms of the bacterial colonies may counteract this increase in density. In addition, model parameterizations do not include spatially-dependent biodegradation rates arising from the response of microbial metabolism to local conditions such as temperature and availability of trace nutrients. For example, droplets are expected to degrade more rapidly as they approach the surface where temperatures are higher. Therefore, the biodegradation rate scenarios likely overestimate the concentration of oil in the upper 400 m where temperatures can range from 10 to 30 °C and, therefore, overestimate the near-surface dispersal of oil. Also, this study applied the degradation rates of alkanes, yet it is likely that droplets also included other crude oil components like aromatic hydrocarbons, asphaltenes and resins. Oil compounds with different molecular weights would dissolve and degrade at different rates, which would also affect droplet density, diameter, and ascent rates. These complexities, which could enhance or decrease dispersal and mass reduction, were not included. Model developments to include parameterizations for many of these processes are underway.

Despite the simplified parameterization in the model presented here, the main result of this sensitivity study, that oil droplet biodegradation rates significantly influence the transport of oil droplets, is robust and indicates that improved information on oil droplet biodegradation is needed for predicting the fate and transport of oil droplets from deep water spills. With better constrained biodegradation rates, this intermediate complexity oil droplet model could be used to identify probable pathways of oil droplet transport from specific locations (after Bourgault *et al* 2014) and thereby provide a screening tool for decision makers who undertake risk analysis and develop contingency plans for subsurface oil spills (Boufadel and Geng 2014).

Acknowledgments

References

Adcroft A, Hallberg R, Dunne J P, Samuels B L, Galt J A, Barker C H and Payton D 2010 Simulations of underwater plumes of dissolved oil in the Gulf of Mexico *Geophys. Res. Lett.* **37** L18605

Bælum J *et al* 2012 Deep-sea bacteria enriched by oil and dispersant from the *Deepwater Horizon* spill *Environ. Microbiol.* **14** 2405–16

Boufadel M C and Geng X 2014 A new paradigm in oil spill modeling for decision making? *Environ. Res. Lett.* **9** 081001

Bourgault D, Cyr F, Dumont D and Carter A 2014 Numerical simulations of the spread of floating passive tracer released at the old harry prospect *Environ. Res. Lett.* **9** 054001

Brandvik P J, Johansen Ø, Leirvik F, Farooq U and Daling P S 2013 Droplet breakup in subsea oil releases: I. Experimental study of droplet breakup and effectiveness of dispersant injection *Mar. Pollut. Bull.* **73** 319–26

Camilli R, Reddy C M, Yoerger D R, Van Mooy B A S, Jakuba M V, Kinsey J C, McIntyre C P, Sylva S P and Maloney J V 2010 Tracking hydrocarbon plume transport and biodegradation at *Deepwater Horizon Science* **330** 201–4

Campo P, Venosa A D and Suidan M T 2013 Biodegradability of corexit 9500 and dispersed South Louisiana crude oil at 5 and 25 °C *Environ. Sci. Technol.* **47** 1960–7

Chan G K Y, Chow A C and Adams E E 2014 Effects of droplet size on intrusion of sub-surface oil spills *Environ. Fluid Mech.* doi:10.1007/s10652-014-9389-5

Chang Y-L, Oey L, Xu F-H, Lu H-F and Fujisaki A 2011 2010 Oil spill—trajectory projections based on ensemble drifter analyses *Ocean Dyn.* **61** 829–39

Commonwealth Scientific and Industrial Research Organization (CSIRO) 2013 Completed dataset from the Commonwealth Scientific and Industrial Research Organization (CSIRO) collected during the response to the Deepwater Horizon incident in the Gulf of Mexico onboard the M/V Ryan Chouest Cruise 1 through Cruise 15 from 2010-06-05 to 2010-09-14 (NODC Accession 0086283). Available online from the US National Oceanographic Data Center (http://accession.nodc.noaa.gov/0086283)

Du M and Kessler J D 2012 Assessment of the spatial and temporal variability of bulk hydrocarbon respiration following the *Deepwater Horizon* oil spill *Environ. Sci. Technol.* **46** 10499–507

(ERMA) Environmental Response Management Application 2014 Web application. Gulf of Mexico, Natural Resources Damage

Assessment, National Oceanic and Atmospheric Administration (http://response.restoration.noaa.gov/erma/)

Hazen T C *et al* 2010 Deep-Sea oil plume enriches indigenous oil-degrading bacteria *Science* **330** 204–8

Hyun K H and He R 2010 Coastal upwelling in the South Atlantic bight: a revisit of the 2003 cold event using long term observations and model hindcast solutions *J. Mar. Syst.* **83** 1–13

Johansen Ø, Brandvik P J and Farooq U 2013 Droplet breakup in subsea oil releases: II. Predictions of droplet size distributions with and without injection of chemical dispersants *Mar. Pollut. Bull.* **73** 327–35

Johansen Ø, Rye H and Cooper C 2003 DeepSpill—field study of a simulated oil and gas blowout in deep water *Spill Sci. Technol. Bull.* **8** 433–43

Joung D and Shiller A 2013 Trace element distributions in the water column near the *Deepwater Horizon* well blowout *Environ. Sci. Technol.* **47** 2161–8

Kessler J D *et al* 2011 A persistent oxygen anomaly reveals the fate of spilled methane in the deep Gulf of Mexico *Science* **331** 312–5

Kujawinski E B, KidoSoule M C, Valentine D L, Boysen A K, Longnecker K and Redmond M C 2011 Fate of dispersants associated with the *Deepwater Horizon* oil spill *Environ. Sci. Technol.* **45** 1298–1306

Lee K and Ryan S 2010 Laser *in situ* Scattering and Transmissometer measurements and supporting data collected in response to the *Deepwater Horizon* oil spill incident from April through August 2010, NODC Accession Number 0086284 (http://accession.nodc.noaa.gov/0086284)

Lehr W, Bristol S and Possolo A 2010 Oil Budget Calculator— *Deepwater Horizon*, Federal Interagency Solutions Group, Oil Budget Calculator Science and Engineering Team (www.crrc.unh.edu/publications/OilBudgetCalcReport_Nov2010.pdf)

Lindo-Atichati D, Paris C B, LeHénaff M, Schedler M, Valladares Juárez A G and Müller R 2014 Simulating the effects of droplet size, high pressure biodegradation, and variable flow rate on the subsea evolution of deep plumes from the Macondo blowout *Deep-Sea Res.* II doi:10.1016/j.dsr2.2014.01.011

Loomis N 2011 Computational imaging and automated identification for aqueous environments *PhD Thesis* Cambridge, MA (MIT and WHOI Joint Program) http://dspace.mit.edu/handle/1721.1/67589

Mariano A J, Halliwell G R, Kourafalou V, Ryan E, Srinivasan A and Roffer M 2011 On the modeling of the 2010 Gulf of Mexico oil spill *Dyn. Atmos. Oceans* **52** 322–40

McNutt M, Camilli R, Guthrie G, Hsieh P, Labson V, Lehr B, Maclay D, Ratzel A and Sogge M 2011 Assessment of flow rate estimates for the Deepwater Horizon/Macondo Well oil spill Flow Rate Technical Group report to the National Incident Command, Interagency Solutions Group (10 March 2011) (www.doi.gov/deepwaterhorizon/loader.cfm?csModule=security/getfile&PageID=237763)

Montagna P A, Baguley J G, Cooksey C, Hartwell I, Hyde L J, Hyland J L, Kalke R D, Kracker L M, Reuscher M and Rhodes A C E Deep-sea benthic footprint of the *Deepwater Horizon* blowout *PLoS One* **8** e70540

Murawski S A, Hogarth W T, Peebles E B and Barbeiri L 2014 Prevalence of fish diseases in the Gulf of Mexico post-Deepwater Horizon *Trans. Am. Fish. Soc.* **143** 1084–97

Nagamine S I 2014 The effects of chemical dispersants on buoyant oil droplets *Master of Science, Dept. of Mechanical Engineering* (Honolulu, HI: University of Hawaii)

NOAA/NOS Office of Response and Restoration 2013 Collection of scribe databases compiled in response to the *Deepwater Horizon* oil spill incident in the Gulf of Mexico from 04/23/2010 to 11/08/2011 NODC Accession 0086261 (http://accession.nodc.noaa.gov/0086261)

North E W, Adams E E, Schlag Z, Sherwood C R, He R, Hyun K H and Socolofsky S A 2011 Simulating oil droplet

dispersal from the *Deepwater Horizon* spill with a Lagrangian approach *Monitoring and Modeling the Deepwater Horizon Oil Spill: A Record-Breaking Enterprise* (Geophys. Monogr. Ser. vol **195**) ed Y Liu *et al* (Washington DC: AGU) pp 217–26

Paris C B, Le Hénaff M, Aman Z, Subramanian A, Wang D-P, Helgers J, Kourafalou V and Srinivasan A 2012 Evolution of the subsea oil from the Macondo well blowout: simulating the effects of the circulation and synthetic dispersants on the subsea oil transport *Environ. Sci. Technol.* **46** 13293–302

Prince R C, McFarlin K M, Butler J D, Febbo E J, Wang F C Y and Nedwed T J 2013 The primary biodegradation of dispersed crude oil in the sea *Chemosphere* **90** 521–6

Reddy C M *et al* 2012 Composition and fate of gas and oil released to the water column during the *Deepwater Horizon* oil spill *Proc. Natl Acad. Sci. USA* **109** 20229–34

Redmond M C and Valentine D L 2012 Natural gas and temperature structured a microbial community response to the *Deepwater Horizon* oil spill *Proc. Natl Acad. Sci. USA* **109** 20292–7

Ryerson T B *et al* 2011 Atmospheric emissions from the *Deepwater Horizon* spill constrain air–water partitioning, hydrocarbon fate, and leak rate *Geophys. Res. Lett.* **38** 1944–8007

Ryerson T B *et al* 2012 Chemical data quantify *Deepwater Horizon* hydrocarbon flow rate and environmental distribution *Proc. Natl Acad. Sci. USA* **109** 20246–53

Socolofsky S A, Adams E E and Sherwood C R 2011 Formation dynamics of subsurface hydrocarbon intrusions following the *Deepwater Horizon* blowout *Geophy. Res. Lett.* **38** L09602

Thessen A E *et al* 2014 GISR Deepwater Horizon Database, Version 1.0. (http://gisr.hpl.umces.edu)

US Coast Guard Dept. of Transportation 1993 Federal on scene coordinator's report: T/V Exxon Valdez oil spill, Vol **1**, Washington DC, pp 599 (www.arlis.org/docs/vol1/B/31206602/31206602v1.pdf)

Valentine D L, Burch Fisher G, Bagby S C, Nelson R K, Reddy C M, Sylva S P and Woo M A 2014 Fallout plume of submerged oil from Deepwater Horizon *Proc. Natl Acad. Sci. USA* **111** 15906–11

Valentine D L, Mezić I, Maćešić S, Črnjarić-Žic N, Ivić S, Hogan P J, Fonoberov V A and Loire S 2012 Dynamic autoinoculation and the microbial ecology of a deep water hydrocarbon irruption *Proc. Natl Acad. Sci. USA* **109** 20286–91

Valentine D L *et al* 2010 Propane respiration jump-starts microbial response to a deep oil spill *Science* **330** 208–11

Venosa A D and Holder E L 2007 Biodegradability of dispersed crude oil at two different temperatures *Mar. Pollut. Bull.* **54** 545–53

Vilcáez J, Li L and Hubbard S S 2013 A new model for the biodegradation kinetics of oil droplets: application to the *Deepwater Horizon* oil spill in the Gulf of Mexico *Geochem. Trans.* **14** 4

Weber T C, De Robertis A, Greenaway S F, Smith S, Mayer L and Rice G 2012 Estimating oil concentration and flow rate with calibrated vessel-mounted acoustic echo sounders *Proc. Natl Acad. Sci. USA* **109** 20240–5

Weisberg R H, Zheng L and Liu Y 2011 Tracking subsurface oil in the aftermath of the *Deepwater Horizon* well blowout *Monitoring and Modeling the Deepwater Horizon Oil Spill: A Record-Breaking Enterprise* (Geophys. Monogr. Ser. vol **195**) ed Y Liu *et al* (Washington DC: AGU) pp 205–15

Weisberg R H, Zheng L, Liu Y, Murawski S, Hu C and Paul J 2014 Did Deepwater Horizon hydrocarbons transit to the west Florida continental shelf? *Deep-Sea Res.* II doi:10.1016/j.dsr2.2014.02.002

Yapa P D and Chen F 2004 Behavior of oil and gas from deepwater blowouts *J. Hydraul. Eng.* **130** 540–53

Yapa P D, Wimalaratne M R, Dissanayake A L and DeGraff J A Jr 2012 How does oil and gas behave when released in deep water? *J. Hydro-environ. Res.* **6** 275–85

Zheng L and Yapa P 2000 Buoyant velocity of spherical and nonspherical bubbles/droplets *J. Hydraul. Eng.* **126** 852–4